Liquid Crystals
Publication details, including instructions for authors and subscription information:
http://www.informaworld.com/smpp/title~content=t713926090

Angular dependence of ^{2}H-NMR longitudinal spin relaxation in aligned nematic 4-n-pentyl-4'-cyanobiphenyl: molecular rotation and director fluctuations

Mario Cifelli[a]; Diego Frezzato[b]; Geoffrey R. Luckhurst[c]; Giorgio J. Moro[b]; Akihiko Sugimura[d]; Carlo A. Veracini[a]
[a] Dipartimento di Chimica e Chimica Industriale, Università di Pisa, Pisa, Italy [b] Dipartimento di Scienze Chimiche, Università degli Studi di Padova, Padova, Italy [c] School of Chemistry, University of Southampton, Highfield, Southampton, UK [d] School of Information Systems Engineering, Osaka Sangyo University, Daito-Shi, Osaka, Japan

Online publication date: 06 July 2010

To cite this Article Cifelli, Mario , Frezzato, Diego , Luckhurst, Geoffrey R. , Moro, Giorgio J. , Sugimura, Akihiko and Veracini, Carlo A.(2010) 'Angular dependence of ^{2}H-NMR longitudinal spin relaxation in aligned nematic 4-n-pentyl-4'-cyanobiphenyl: molecular rotation and director fluctuations', Liquid Crystals, 37: 6, 773 — 784
To link to this Article: DOI: 10.1080/02678292.2010.492108
URL: http://dx.doi.org/10.1080/02678292.2010.492108

Liquid Crystals,
Vol. 37, Nos. 6–7, June–July 2010, 773–784

Taylor & Francis
Taylor & Francis Group

INVITED ARTICLE

Angular dependence of ^{2}H-NMR longitudinal spin relaxation in aligned nematic 4-n-pentyl-4'-cyanobiphenyl: molecular rotation and director fluctuations

Mario Cifelli[a], Diego Frezzato[b]*, Geoffrey R. Luckhurst[c], Giorgio J. Moro[b], Akihiko Sugimura[d] and Carlo A. Veracini[a]

[a]*Dipartimento di Chimica e Chimica Industriale, Università di Pisa, Pisa, Italy;* [b]*Dipartimento di Scienze Chimiche, Università degli Studi di Padova, Padova, Italy;* [c]*School of Chemistry, University of Southampton, Highfield, Southampton, UK;* [d]*School of Information Systems Engineering, Osaka Sangyo University, Daito-Shi, Osaka, Japan*

(*Received 31 March 2010; accepted 4 May 2010*)

The longitudinal (spin-lattice) relaxation in nuclear magnetic resonance (NMR) experiments on 4-n-pentyl-4'-cyanobiphenyl (5CB) mesogen, deuteriated in the alpha-position, has been investigated by changing the orientation of the phase director with respect to the instrumental magnetic field through the application of a competing alternating electric field. The angular-dependent profiles of the corresponding rotational spectral densities were fitted and interpreted by invoking a model for single-molecule reorientational dynamics and fluctuations of the local director with respect to the average direction of alignment. The relative contribution of the two processes to the longitudinal relaxation rate has been estimated, and values of the principal components of the rotational diffusion tensor of the 5CB molecule were obtained from the data fit. The work focuses mainly on the methodological grounds, by pointing out the increase in the extent of achievable information when passing from standard NMR experiments performed at the canonical orientation of the sample (that is an alignment collinear to the magnetic field) to measurements on arbitrarily oriented samples.

Keywords: nematic; director fluctuations; molecular rotation; spin relaxation; anisotropy

1. Introduction

In recent decades, dynamics in thermotropic liquid crystals, which span a range from fast single-molecule motions up to much slower collective processes like the fluctuations of the local orientational director, have attracted the attention of researchers [1]. There are several reasons for this. First, from the academic point of view, since these are stochastic processes which take place in anisotropic fluid environments, hence they offer the possibility to validate and refine the theoretical modelling. Secondly, because dynamics offer the possibility to probe the ordering properties in the phase, indirectly. Finally, in view of technical applications and the design of materials, since the dynamics at equilibrium are related to the macroscopic response of the sample when external stimuli are applied.

Several spectroscopic techniques have been employed to study dynamics in liquid crystals and amongst them nuclear magnetic resonance (NMR) is considered a powerful and versatile means for this purpose. In particular, deuterium NMR plays an important role because the spectra of specifically deuteriated mesogens are rather simple to interpret compared with the corresponding proton NMR spectra [2]. The quadrupolar splitting observed in liquid crystal phases is directly related to the orientational order of the C–D bond and its alignment with the magnetic field direction, and so provides a powerful means to study the molecular order, structure and phase transitions in liquid crystal phases. Furthermore, investigation of the ^{2}H-NMR relaxation processes driven by modulation of the Zeeman and quadrupolar interactions, namely the measurement of transverse and longitudinal relaxation times, is a well-established technique to study molecular dynamics in liquid crystals [3, 4]. In fact, in the limit of a fast-motional treatment of NMR relaxation [5, 6], the relaxation rates can be related to spectral densities of specific second-rank correlation functions for the reorientational dynamics of the spin-probe molecule; these are, generally speaking, fast internal conformational transitions [7], slower rotational diffusive motions (tumbling and spinning) of the molecule as a whole in the anisotropic environment [8], and even slower fluctuations of the local orientational director [9].

As the spectral densities contain, even though in an implicit way, all of the information needed to investigate the rotational molecular dynamics, or better those molecular dynamics that affect the specific relaxation process under investigation, their measurement is a key approach for the study of molecular motion in liquid

*Corresponding author. Email: diego.frezzato@unipd.it

ISSN 0267-8292 print/ISSN 1366-5855 online

DOI: 10.1080/02678292.2010.492108
http://www.informaworld.com

crystals. In fact, NMR relaxation experiments normally provide limited information on the spectral densities as long as the measurement is made at a single frequency and at a single orientation of the phase director with respect to the magnetic field. This condition can strongly limit the amount of achievable information; in particular, it has been shown that limited experimental data sets could be insufficient to determine the rotational diffusion coefficients unambiguously [10].

The former limitation can be overcome by working at different frequencies, that is by exploiting different NMR spectrometers [11] or resorting to NMR relaxometry [12], while overcoming the latter constraint is indeed more complicated. The orientation of the phase director by the magnetic field depends on both the diamagnetic anisotropy, $\Delta\chi$, and the magnetic field strength. In the case of positive $\Delta\chi$, the phase director aligns parallel to the magnetic field; this is the canonical orientation for calamitic mesogens forming nematic and smectic A phases. In principle, we can rotate the director away from the magnetic field direction by rotating the whole sample exploiting, for example, a goniometer probe. This approach has been used successfully in the smectic B [13] and smectic A [14] phases of calamitic mesogens. In these cases, the phase director was uniformly aligned in the nematic phase which was then cooled into the smectic phases. As no phase director realignment was observed under sample rotation of a smectic sample, relaxation measurements could be undertaken at different angles between the phase director and the static magnetic field. As far as a nematic phase is concerned, sample rotation is not feasible as backflow is very efficient due to the low phase viscosity. An alternative is to rotate the phase director by exploiting an electric field of suitable strength and orientation. In this case, the magnetic torque is balanced by the electric one, and the phase director can be kept at an arbitrary angle with respect to the magnetic field. This use of DC/AC electric fields competing with the magnetic field has been exploited in the past to measure the proton longitudinal relaxation time in oriented nematic phases of low molecular weight mesogens possessing positive or negative dielectric anisotropies [15, 16]. At that time the problem was raised that longitudinal relaxation may be affected by induced turbulence when low-frequency alternating electric fields (few tens of kHz) are employed. More recently, a combination of magnetic and electric torques have been used by Sugimura and co-workers to study the static director alignment as well as the field-induced director dynamics by means of deuterium NMR. Several aspects and achievements of this work have been reviewed recently by Luckhurst *et al.* [17].

In this paper we describe the application of an analogous approach to measure the longitudinal relaxation times T_{1Z} (Zeeman term) and T_{1Q} (quadrupolar term) for different director orientations in the nematic phase of a calamitic nematogen, namely 4-n-pentyl-4'-cyanobiphenyl (5CB). The magnetic and dielectric anisotropies, $\Delta\chi$ and $\Delta\varepsilon$, respectively, for this nematogen are both positive. The sample, confined in a cell formed by two glass plates, is connected to a function generator and a high-power amplifier. The cell is inserted in the magnetic field of the spectrometer and can also be subject to an electric field perpendicular to the glass plates. As the electric field is increased, so the director moves from being parallel to the magnetic field to being parallel to the electric field. Accordingly, the introduction of an electric torque into the NMR experiment allows the relaxation times (and hence the spectral densities) to be measured as a function of the resulting angle between the director and the magnetic field. This increases the information content of the experiment and so enables a more sensible data fit, once a theoretical model for the relevant dynamics of 5CB is adopted.

The layout of the paper is as follows. The next Section describes the ^{2}H-NMR experiment and the equipment, and Section 3 gives the theoretical description of the longitudinal relaxation process which we consider. In Section 4 the methodological tools are applied to fit the experimental data and the results are interpreted. In Section 5 we draw our conclusion and suggest further work.

2. Experimental setup for ^{2}H-NMR in aligned nematic 5CB

The sample used for the NMR experiments was 5CB specifically deuteriated on the alpha position of the alkyl chain. The nematic–isotropic transition was found at 31°C, which is lower than the value usually reported for this nematogen [18]. The difference can be ascribed to the presence of a small amount of impurities due to sample aging under the effect of several cycles of experiments, for example, partial leaking of the sealing glue into the sample. Nevertheless, it can be noted that the sample fully preserves its nematic behaviour and could also be supercooled in the nematic phase down to 5°C. All of the measurements have been carried out on a JEOL ECA-300 spectrometer, with a magnetic flux intensity of 7.05 T, corresponding to a deuterium Larmor frequency of 46 MHz. In order to apply an electric field, a nematic sandwich cell, 150 μm thick, was prepared from glass plates coated with In_2O_3 to act as the electrodes, as described elsewhere [17]. The sample cell was held in the probe head so that the electric field direction (perpendicular to the glass plates) could be freely rotated with respect to the magnetic field as sketched in Figure 1. This was achieved with a

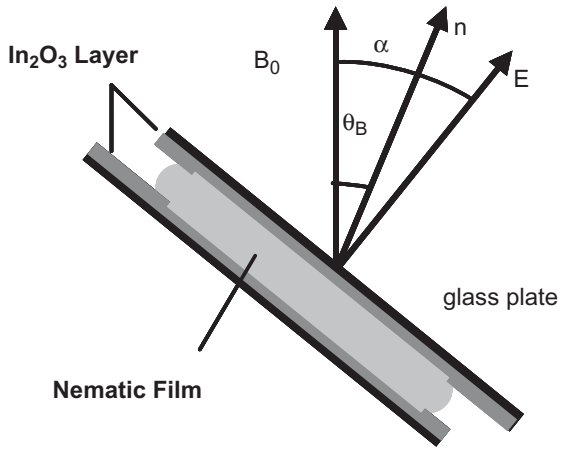

Figure 1. Sample geometry as discussed in the text, shown here for an arbitrary equilibrium tilt angle θ_B resulting from a combination of magnetic and electric field torques. The sandwich cell, 150 μm thick, was inserted in a solenoid coil, 10 mm internal diameter, in the NMR spectrometer and the In_2O_3 electrodes were connected to the electric wave generator/amplifier through shielded electric wires.

goniometer controlled by an ultrasonic stepping motor to allow rotation of the sample cell about an axis perpendicular to the magnetic field; the goniometer allows the variation of the angle, α, between the electric field and the static magnetic field $\mathbf{B_0}$ (see Figure 1).

To apply the electric field, a high-power amplifier (model 4005 NF Electronic Instruments) and a function generator (Wave Factory WF1943, NF Electronic Instruments) were connected to the sample cell, providing a sinusoidal 1–10 kHz AC electric field with a maximum average potential of $200V_{rms}$. For the present experiment a 5 kHz electric field was applied. This frequency was sufficient to avoid possible ionic conduction and so to produce uniform alignment of the director [19].

The 90° pulse width was calibrated to 7.7 μs and the longitudinal relaxation times, namely the Zeeman and quadrupolar order relaxation times, T_{1Z} and T_{1Q}, were measured by exploiting a broad-band variation of the Jeener–Broekaert echo proposed by Wimperis [20]:

$$90^\circ_x - t_q - 67.5^\circ_{-y} - t_q - 45^\circ_y - t_q/2 - 45^\circ_y - t_{var} - \delta_x - acq.$$

The delay, t_q, has been adjusted in the experiment to produce the best anti-phase quadrupolar doublet when t_{var}vanishes, while the δ-pulse was set to 45° in order to maximise the quadrupolar order just before the acquisition. Spectra were acquired by accumulating from 2000 to 8000 FIDs for a good signal-to-noise ratio to ensure reliable integration of the peaks of the quadrupolar doublet. The variable delay, t_{var}, was increased from 10 μs to 500 ms and the sum (M_+) and the difference (M_-) of the integrals of the components of the quadrupolar doublet, reported as a function of the variable delay, have been used to obtain T_{1Z} and T_{1Q} respectively, by fitting them with the two equations:

$$M_+(t_{var}) = c_1\left(1 - \exp\left(\frac{t_{var}}{T_{1Z}}\right)\right) + c_2 \qquad (1a)$$

and

$$M_-(t_{var}) = c_3 \exp\left(\frac{t_{var}}{T_{1Q}}\right) + c_4. \qquad (1b)$$

The parameters c_1, c_2, c_3, c_4 were allowed to float in order to compensate for deviations from the theoretical behaviour which implies a complete magnetisation inversion when $t_{var} = 0$ and $c_2 = 1$, $c_4 = 0$. In all the fittings the best values for c_2 were in the range 1 ± 0.04 and c_4 in the range $\pm 1\%$ of the c_3 value extrapolated to $t_{var} = 0$. A recycle delay of 0.6 s was chosen to be at least five times the expected T_1 values, in order to ensure complete relaxation between each FID during the acquisitions. An example of the experimental data collected at one temperature and their fitting with Equations (1a) and (1b) is reported in Figure 2.

The relaxation measurements were made at three different temperatures, namely 25°C, 15°C and 6°C, obtained by cooling the sample from the isotropic phase. The temperature stability was better than ± 0.2°C. In order to exploit the angular dependence of the longitudinal relaxation processes for the investigation of molecular and director dynamics, measurements were repeated at different orientations of the director with respect to the magnetic field.

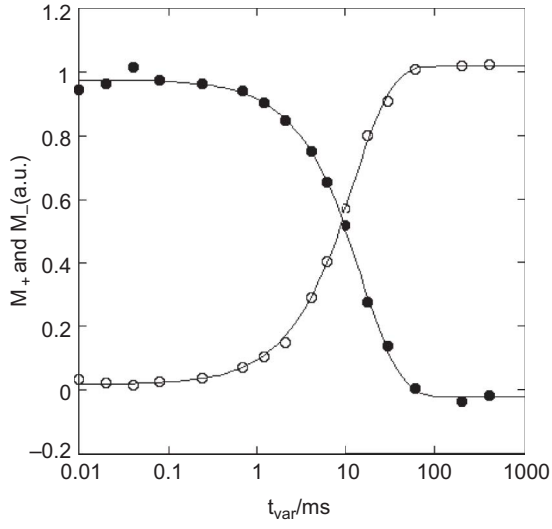

Figure 2. Sum (○) and difference (●) of the intensities of the two components for the quadrupolar splitting as a function of the variable time, t_{var}, measured at 15°C and θ_B = 85° (logarithmic scale). The recovery and decay of the magnetisation have been fitted with Equations (1a) and (1b), respectively. Relevant fit parameters are $c_1 = c_3 = 1$, $c_2 = 0.02$ and $c_4 = 0.01$ leading to $T_{1Z} = 15.6$ ms and $T_{1Q} = 12.47$ ms.

The sample alignment was obtained and determined in the following way. The sample cell was inserted in the goniometer probe with an initial value of the angle α set to be about 20° (a clockwise rotation with respect to the magnetic field direction). The sample was heated into the isotropic phase and then cooled into the nematic phase. A monodomain was formed with the average director parallel to the magnetic field ($\theta_B = 0$) and the quality of the alignment was checked by acquiring the spectrum with a quadrupolar echo sequence (τ = 30 μs delay between the two 90° pulses, 400 FIDs). A single quadrupolar splitting, $\Delta\nu_0$, was obtained, indicating a uniform alignment of the director for the whole sample. The splitting, measured at 25°C, was 52.13 kHz, and can be expressed as

$$\Delta\nu_0 = \frac{3}{2} q_{CD} S^0_{CD}. \tag{2}$$

Here $q_{CD} = e^2Qq/h$ is the quadrupolar coupling constant for the deuteron in the specific chemical site and S^0_{CD} is the second-rank orientational order parameter of the C–D bond with reference to the phase director which in a zero electric field is parallel to the magnetic field. Relaxation times have then been measured at this orientation, giving the canonical spin relaxation times, T_{1Z} and T_{1Q}, usually measured in relaxation studies.

The electric field was then applied. From the competition between the magnetic and electric torques, equilibrium is established with the phase director aligned at an angle θ_B with respect to the magnetic field. When the two torques are balanced, the theory gives the angle made by the director with the magnetic field, as described elsewhere [17]:

$$\cos 2\theta_B = \frac{1 + \rho \cos 2\alpha}{\sqrt{(1 + 2\rho \cos 2\alpha + \rho^2)}}. \tag{3}$$

Here ρ is the ratio of the electric and magnetic anisotropic energies, U_e and U_m, respectively:

$$\rho = \frac{U_e}{U_m} = \mu_0 \varepsilon_0 \left(\frac{E}{B_0}\right)^2 \left(\frac{\Delta\varepsilon}{\Delta\chi}\right),$$
$$U_m = \frac{\Delta\chi}{2\mu_0} B_0^2, \quad U_e = \frac{\varepsilon_0 \Delta\varepsilon}{2} E^2. \tag{4}$$

The resulting angle depends on parameters related to the properties, $\Delta\chi$ and $\Delta\varepsilon$, of the liquid crystal but also on the magnetic and electric field strengths and the angle, α, between the two fields. In the limit that the applied electric field is sufficiently high, that is if $U_e >> U_m$, the expression in Equation (3) reduces to

$$\cos 2\theta_B \approx \cos 2\alpha. \tag{5}$$

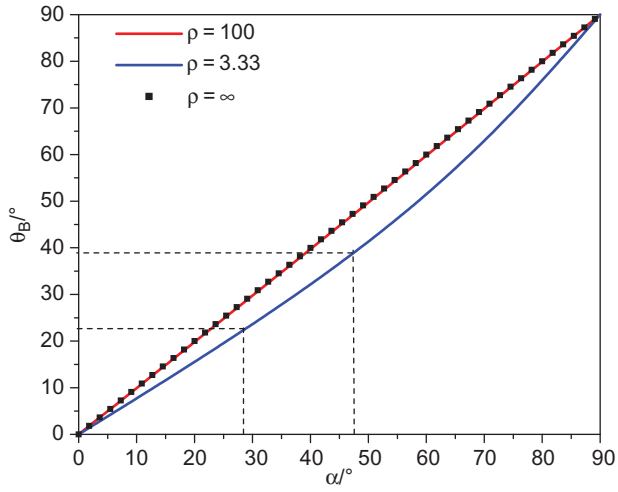

Figure 3. Calculated relationship between α and θ_B as a function of ρ. As shown in the figure a director alignment practically independent of the magnetic field could be achieved for $\rho \geq 100$. For the experimental condition considered in the text ($\rho = 3.33$) $\alpha > \theta_B$ for $0 < \alpha < 90°$.

Now a uniform alignment of the director parallel to the electric field is obtained with $\theta_B = \alpha$. In practice, however, this condition is not easily fulfilled. As shown in Figure 3, the ratio ρ should be greater than 100 to achieve a difference between α and θ_B of less than 0.5° over a range 0°–90°.

At the maximum electric field applicable to the sample cell (180 V_{rms}), considering average values of $\Delta\varepsilon = 10$ and $\Delta\chi = 10^{-6}$ for the 5CB sample in the nematic phase [17] and the sample cell thickness, we can estimate that ρ is just 3.3 (see Figure 3). For this relatively small value Equation (5) could not be applied. Consequently, even though the orientation of the phase director was varied by rotating the sample using the probe goniometer, the precise evaluation of θ_B was determined by measuring the quadrupolar splitting from the spectrum. A single splitting corresponding to a monodomain was always obtained, and θ_B was evaluated from the equation [17]

$$\Delta\nu = \Delta\nu_0 \left(\frac{3\cos^2\theta_B - 1}{2}\right). \tag{6}$$

Keeping the electric field on, different θ_B angles were obtained by rotating the sample with the goniometer and the spin relaxation times $T_{1Z}(\theta_B)$ and $T_{1Q}(\theta_B)$ were then measured at 25°C. This procedure was repeated at the two lower temperatures of 15°C ($\Delta\nu_0$ = 60.67kHz) and 6°C ($\Delta\nu_0$ = 63.30kHz). The entire angular dependences of the relaxation times measured for the three temperatures are shown in Figure 4. The uncertainties in the relaxation times, ΔT_{1Z} and ΔT_{1Q}, were estimated by

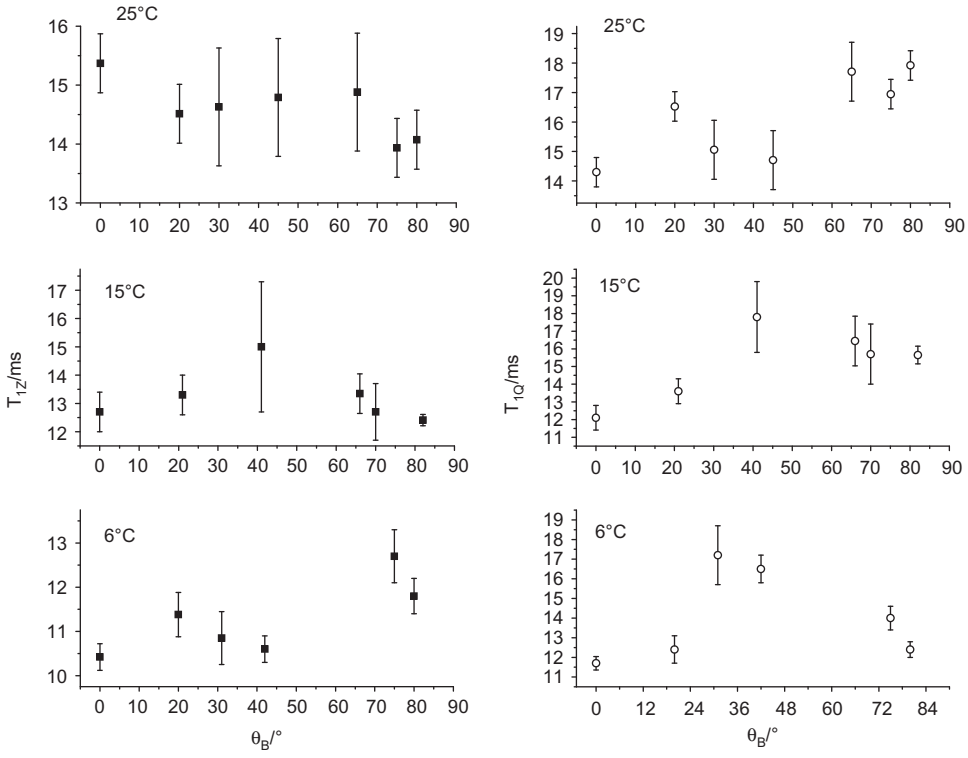

Figure 4. The spin longitudinal relaxation times T_{1Z} (filled squares, left panels) and T_{1Q} (open circles, right panels) measured for different director orientations. The error bars reported are the uncertainties obtained from a non-linear fitting procedure of the experimental decays and recoveries of the magnetisation as t_{var} increases.

the non-linear fitting of the experimental decays and recoveries of the magnetisation. We mention that the present outcomes compare well with previous estimates of rotational spectral densities from NMR at the canonical orientation for 5CB deuteriated in the alpha position of the alkyl chain [21, 22]. For example, using data in Table 2 of Counsell *et al.* [22], which are for experiments 4.8 K below the nematic–isotropic phase transition and at a resonance frequency of 30.7 MHz, we obtain $T_{1Q} = (0.0146 \pm 0.0012)$ s and $T_{1Z} = (0.0137 \pm 0.0009)$ s; these values are comparable with the present estimates $T_{1Q} = (0.0143 \pm 0.0005)$ s and $T_{1Z} = (0.0154 \pm 0.0005)$ s at 25°C but at the higher frequency of 46 MHz. As shown in Counsell *et al.* [22], an increase of the Larmor frequency causes a reduction in the spectral densities, which means an increase of the relaxation times. Such a trend may justify the larger value of T_{1Z} that we find here at 46 MHz, while T_{1Q} appears to be much less sensitive to the change of frequency.

3. Theoretical description of the longitudinal relaxation in the aligned nematic

Our goal is to set up a *minimal* model for the dynamics of the molecules in the nematic phase, which may be able to interpret the experimental measurements with as small a number of free parameters as possible (to obtain a sensible data-fit), but still able to catch the physical features in a realistic way.

In the analysis of the *longitudinal* relaxation we shall ignore the possible contribution of intramolecular dipolar interactions between the two deuterons, which is assumed to be negligible compared with that of the dominant quadrupolar and Zeeman interactions. As a matter of fact, this starting assumption is verified *a posteriori* on the basis of the good fit of the theory to the spin relaxation data, as we shall see. However, dipolar interactions may play a relevant role in driving the *transverse* relaxation, since they are dynamically coupled to the other interactions determining the spectral linewidths; their possible relevance has been highlighted in variable delay quadrupolar echo experiments, where a regular modulation appears in the decay of the quadrupolar echo intensity versus the pulse-spacing [23]. Moreover, since the two deuterons are equivalent, and taken as decoupled in our model, we may focus only on one of them.

The analysis of the contributions to the longitudinal relaxation rate T_1^{-1} due to quadrupolar (T_{1Q}^{-1}) and Zeeman (T_{1Z}^{-1}) interactions, can be made by adopting the standard Redfield (fast-motional) approach [5, 6, 24]. The basic theory relates the relaxation rates to the second-rank rotational spectral densities $J_1(\theta_B, \omega_0)$

and $J_2(\theta_B, 2\omega_0)$, which here depend on the angle θ_B, with ω_0 denoting the Larmor frequency,

$$\begin{aligned} T_{1Q}^{-1} &= 3K_Q J_1(\theta_B, \omega_0), \\ T_{1Z}^{-1} &= K_Q[J_1(\theta_B, \omega_0) + 4J_2(\theta_B, 2\omega_0)], \end{aligned} \tag{7}$$

where

$$K_Q = \frac{3\pi^2}{2} {q_{CD}}^2 \tag{8}$$

and the quadrupolar tensor is taken to be cylindrically symmetric about the C–D bond.

In order to specify the required spectral densities we introduce a Laboratory Frame (LF) with the z-axis parallel to the magnetic field and with arbitrary transverse axes. We then consider a Quadrupolar Frame (QF) with the z-axis taken along the C–D bond for the chosen deuteron. We denote the set of Euler angles, defined according to Rose's convention [25], which bring the LF into the QF, by Ω_0. The specific spectral densities are given by:

$$J_i(\theta_B, \omega) = \mathrm{Re}\left\{ \int_0^\infty dt\, e^{-i\omega t} \left\langle \delta D^2_{i,0}(\Omega_0)^*_0\, \delta D^2_{i,0}(\Omega_0)_t \right\rangle \right\}, \quad i = 1, 2 \tag{9}$$

where $\langle \delta D^2_{i,0}(\Omega_0)^*_0\, \delta D^2_{i,0}(\Omega_0)_t \rangle$ are time-correlation functions, $D^2_{i,0}(\Omega_0)$ denote the rotational Wigner functions [25] and $\delta D^2_{i,0}(\Omega_0) = D^2_{i,0}(\Omega_0) - \left\langle D^2_{i,0} \right\rangle$ is their difference from the equilibrium average.

The total transformation from LF to QF is conveniently partitioned into a sequence of rotations between frames that are shown in Figure 5. First, we introduce the Average Director Frame (ADF) whose longitudinal axis is collinear to the phase director of the nematic monodomain, while the transverse axes are arbitrarily chosen. The angle between the z-axes of LF and ADF is θ_B. Then we introduce a local Director Frame (DF) at the point of the sample where the molecule being considered is located, by taking the longitudinal axis along the local instantaneous director in that location while the transverse axes are again arbitrarily chosen. Once a proper Molecular Frame (MF) is adopted, the actual molecular orientation with respect to the DF is specified by the set of Euler angles Ω' while the set of Euler angles which brings ADF to MF is denoted by Ω in the subsequent text. A final internal transformation specifies the orientation of the quadrupolar tensor with respect to the MF. From this set of transformations we see that the motions which drive the relaxation of the spectral signal, i.e. which affect the rotational correlation functions and their spectral densities in Equation (9), may be slow director fluctuations of the local director, global reorientations of the molecule as a whole with respect to the DF axes and internal conformational dynamics.

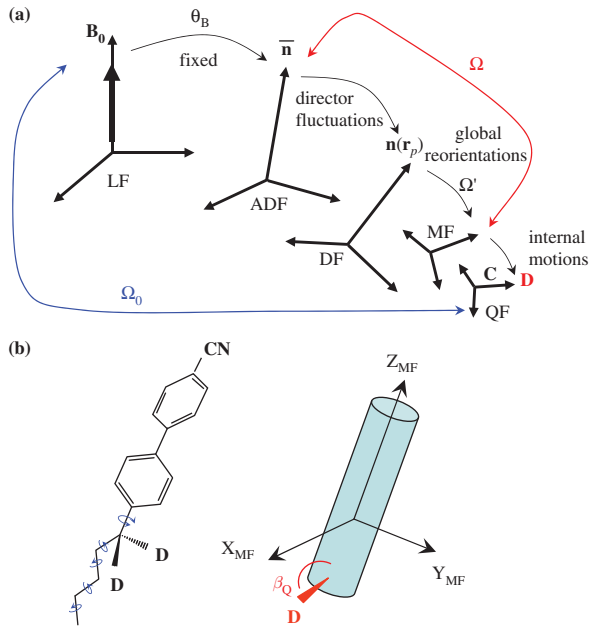

Figure 5. (a) Sequence of reference frames: Laboratory Frame (LF), Average Director Frame (ADF), local Director Frame (DF), Molecular Frame (MF), Quadrupolar Frame (QF). (b) Cylindrical symmetry approximation for the molecule in its conformationally averaged form.

The choice of the MF is based on the assumption that internal motions are so fast in comparison to the timescale of the molecular reorientation [1], such that a time average over the molecular conformations (however made on a time-window shorter than the rotational correlation times) produces a *dynamically averaged conformation*. The MF that we adopt has its z-axis collinear to the molecular symmetry axis in such an average conformation and the x-axis in the plane formed by the z-axis and by the C_α–D bond under consideration. The effective symmetry axis of the molecule in its averaged conformation does not require a rigorous definition here. Based on symmetry arguments for the 5CB molecule, such a symmetry axis is reasonably taken as parallel to the inter-ring C–C bond. Our assumption of uniaxial symmetry for the quadrupolar tensors for the deuterons, means that the final internal transformation is specified by the set of Euler angles $(0, \beta_Q, 0)$, where β_Q is the angle formed by the z-axis of the molecular frame and the C_α–D bonds. Due to geometrical constraints imposed by the molecular structure, we expect β_Q to have a value close to 180°-tetrahedral angle, that is 70.5°.

With reference to such a sequence of frame transformations, we can apply the closure relation for the Wigner functions [25] in order to express $\delta D^2_{i,0}(\Omega_0)_0$ in Equation (9) as a sum of products of Wigner functions

evaluated at the Euler angles for the intermediate rotations. By means of some algebraic steps and rearrangements, we can express J_1 and J_2 in the following compact form:

$$\begin{aligned} J_1(\theta_B,\omega_0) &= j_0(\omega_0)d^2_{1,0}(\theta_B)^2 \\ &\quad + j_1(\omega_0)\left[d^2_{1,1}(\theta_B)^2 + d^2_{1,-1}(\theta_B)^2\right] \\ &\quad + j_2(\omega_0)\left[d^2_{1,2}(\theta_B)^2 + d^2_{1,-2}(\theta_B)^2\right], \\ J_2(\theta_B,2\omega_0) &= j_0(2\omega_0)d^2_{2,0}(\theta_B)^2 \\ &\quad + j_1(2\omega_0)\left[d^2_{2,1}(\theta_B)^2 + d^2_{2,-1}(\theta_B)^2\right] \\ &\quad + j_2(2\omega_0)\left[d^2_{2,2}(\theta_B)^2 + d^2_{2,-2}(\theta_B)^2\right]; \end{aligned} \tag{10}$$

here $d^2_{m,k}(\theta_B)$ are second-rank reduced or small Wigner functions [25], and $j_m(\omega)$ are spectral densities given by:

$$\begin{aligned} j_m(\omega) &= \sum_{m'} d^2_{m',0}(\beta_Q)^2 \\ &\times \mathrm{Re}\left\{\int_0^\infty dt\; e^{-i\omega t}\left\langle \delta D^2_{m,m'}(\Omega)_0{}^* \delta D^2_{m,m'}(\Omega)_t \right\rangle\right\}. \end{aligned} \tag{11}$$

By inserting the explicit forms of the reduced Wigner functions, the spectral densities in Equations (10) can be rearranged in the more familiar expressions where the angular dependence on θ_B is expressed in terms of the second- and fourth-rank Legendre polynomials as:

$$\begin{aligned} J_1(\theta_B,\omega_0) &= A_1^{(0)}(\omega_0) + A_1^{(2)}(\omega_0)\; P_2(\cos\theta_B) \\ &\quad + A_1^{(4)}(\omega_0)\; P_4(\cos\theta_B) \end{aligned}$$

and

$$\begin{aligned} J_2(\theta_B,2\omega_0) &= A_2^{(0)}(2\omega_0) + A_2^{(2)}(2\omega_0)\; P_2(\cos\theta_B) \\ &\quad + A_2^{(4)}(2\omega_0)\; P_4(\cos\theta_B). \end{aligned} \tag{12}$$

The Legendre polynomials are defined by: $P_2(x) = (3x^2 - 1)/2$ and $P_4(x) = (35x^4 - 30x^2 + 3)/8$; the frequency dependent coefficients are given by:

$$\begin{aligned} A_1^{(0)}(\omega_0) &= [j_0(\omega_0) + 2j_1(\omega_0) + 2j_2(\omega_0)]/5 \\ A_1^{(2)}(\omega_0) &= [j_0(\omega_0) + j_1(\omega_0) - 2j_2(\omega_0)]/7 \\ A_1^{(4)}(\omega_0) &= [-12j_0(\omega_0) + 16j_1(\omega_0) - 4j_2(\omega_0)]/35 \\ A_2^{(0)}(2\omega_0) &= [j_0(2\omega_0) + 2j_1(2\omega_0) + 2j_2(2\omega_0)]/5 \\ A_2^{(2)}(2\omega_0) &= [-2j_0(2\omega_0) - 2j_1(2\omega_0) + 4j_2(2\omega_0)]/7 \\ A_2^{(4)}(2\omega_0) &= [3j_0(2\omega_0) - 4j_1(2\omega_0) + j_2(2\omega_0)]/35. \end{aligned} \tag{13}$$

This outcome is consistent with the derivation of Doane *et al.* [16]. Equations (12) are important because they reveal the general form of the angular dependence of the spectral densities and, most important, they show to what extent the information content of the experiment has increased on passing from the standard NMR experiment at the canonical orientation to that with an oriented sample. That is, we go from two independent pieces of information (the single values of $J_1(0,\omega_0)$ and $J_2(0,2\omega_0)$) to six (the three coefficients in the equations for the two spectral densities). We note that similar problems and solutions are found in electron spin resonance (ESR) studies of spin relaxation for nitroxide spin probes dissolved in anisotropic media. Here measurement of the angular dependence of the linewidths produces analogous enhancement of the information content of the experiment [26]. In addition, for certain basic models of the reorientational dynamics the coefficient of the $P_2(\cos\theta_B)$ term is found to depend on the second-rank order parameter while that for the $P_4(\cos\theta_B)$ term is found to depend on the fourth-rank order parameter.

In our simplified model, two dynamical processes may affect the spectral densities $j_m(\omega)$: fast single-molecule rotations and slower so-called collective Order Director Fluctuations (ODF) but better thought of simply as director fluctuations. In the crudest approach these processes may be seen as dynamically decoupled by assuming that they occur on very different timescales, thus giving the additive contributions:

$$j_m(\omega) = j_m(\omega)^{\mathrm{rot}} + j_m(\omega)^{\mathrm{ODF}}. \tag{14}$$

The contribution of director fluctuations, $j_m(\omega)^{\mathrm{ODF}}$, can be easily derived for small-amplitude ODF. In this limit, first-order analysis shows that only $j_1(\omega)$ is affected by the ODF:

$$\begin{aligned} j_1(\omega)^{\mathrm{ODF}} &= 3\; S_{\mathrm{CD}}{}^2\; \gamma(\omega)^{\mathrm{ODF}}, \\ \gamma(\omega)^{\mathrm{ODF}} &= \mathrm{Re}\left\{\int_0^\infty dt\; e^{-i\omega t}\langle n_\perp(0) n_\perp(t)\rangle\right\}, \end{aligned} \tag{15}$$

where $n_\perp$ is the transverse component of the instantaneous director in the plane orthogonal to the average director, and S_{CD} is the second-rank order parameter of the C–D bond with respect to the local director. The explicit form of the function $\gamma(\omega)^{\mathrm{ODF}}$ in Equation (15) has been given and discussed in many papers [24, 27, 28]. In short, it is given by:

$$\gamma(\omega)^{\mathrm{ODF}} = w\frac{1}{\sqrt{\omega_0}}U(\omega_c/\omega_0), \quad w = \frac{k_B T}{4\pi\sqrt{2}}\left(\frac{\eta_{\mathrm{eff}}}{K^3}\right)^{1/2}, \tag{16}$$

where η_{eff} is an effective viscosity and K is an average elastic constant for the nematic liquid crystal, ω_c is the cut-off frequency of the ODF modes (to be evaluated from $\omega_c = (K/\eta_{\text{eff}})(2\pi/\lambda_c)^2$ with λ_c the so-called short-length cut-off), and $U(x)$ is the cut-off function

$$U(x) = \frac{1}{2\pi}\ln\left[\frac{x-\sqrt{2x}+1}{x+\sqrt{2x}+1}\right] + \frac{1}{\pi}\left[\arctan(\sqrt{2x}-1)+\arctan(\sqrt{2x}+1)\right]. \tag{17}$$

Now we shall consider in more detail the contribution $j_m(\omega)^{\text{rot}}$ from molecular rotations. In the limit of small-amplitude ODF, the rotational contribution can be approximated by adopting an expression like Equation (11) where Ω is replaced by Ω'. To evaluate the rotational time-correlation function, we have to adopt a model for the stochastic reorientations of the Molecular Frame with respect to the Director Frame. Here we assume small-step diffusive rotational dynamics of the molecule in the local molecular-field potential of mean torque. The stochastic dynamics is described by the Smoluchowski equation [29], whose solution gives the evolution of the conditional probability distribution $p(\Omega'|\Omega'_0, t)$ with the initial condition $p(\Omega'|\Omega'_0, 0) = \delta(\Omega' - \Omega'_0)$ and stationary limit $\lim_{t\to\infty} p(\Omega'|\Omega'_0, t) = p_{\text{eq}}(\Omega')$, where $p_{\text{eq}}(\Omega')$ is the Boltzmann distribution function at thermal equilibrium. The Smoluchowski equation is:

$$\frac{\partial}{\partial t}p(\Omega'|\Omega'_0, t) = -\hat{\Gamma}_{\Omega'}p(\Omega'|\Omega'_0, t), \qquad \hat{\Gamma}_{\Omega'} = -\nabla_{\Omega'}\cdot\mathbf{D}p_{\text{eq}}(\Omega')\nabla_{\Omega'}p_{\text{eq}}(\Omega')^{-1}, \tag{18}$$

where $\mathbf{D}$ is the molecular rotational diffusion tensor expressed with reference to the Molecular Frame axes, and $\nabla_{\Omega'}$ is the gradient operator in the rotational variables [25]. Once Equation (18) is solved formally with respect to $p(\Omega'|\Omega'_0, t)$, the required time-correlation functions are evaluated as:

$$\left\langle \delta D^2_{m,m'}(\Omega')_0{}^*\delta D^2_{m,m'}(\Omega')_t \right\rangle = \int d\Omega' \int d\Omega'_0\, p_{\text{eq}}(\Omega'_0) \times p(\Omega'|\Omega'_0, t)\delta D^2_{m,m'}(\Omega')^*\delta D^2_{m,m'}(\Omega'_0) \equiv \int d\Omega'\, \delta D^2_{m,m'}(\Omega')^* e^{-\hat{\Gamma}_{\Omega'}t}p_{\text{eq}}(\Omega')\delta D^2_{m,m'}(\Omega'). \tag{19}$$

Standard methodologies [1] employed to evaluate the expression in Equation (19) make use of (i) symmetrisation of the integral, (ii) expansion in an ortho-normal basis set of functions (normalised Wigner functions) which span the space of continuous rotations, in order to achieve a matrix representation of the integral, and (iii) exploitation of an eigenvector/eigenvalue analysis.

The equilibrium orientational distribution function is modelled here by taking the following P_2-like form for the potential of mean torque for a uniaxial molecule in a uniaxial phase:

$$V(\Omega')/k_BT = \varepsilon\left(3\cos^2\beta - 1\right)/2. \tag{20}$$

Here β is the angle between the z-axis of the MF and the local director, and $\varepsilon < 0$ is a parameter which determines the strength of the orientational ordering. In the following, $\langle P_2\rangle = \langle P_2(\cos\beta)\rangle$ denotes the second-rank order parameter of the z-axis of the MF with reference to the local director. This choice for the potential, V(Ω'), is equivalent to adopting the basic Maier–Saupe molecular-field theory of uniaxial nematics [19]. This one-parameter model is the most convenient and quite realistic choice for the interpretation of relaxation data which depend only indirectly on the features of the orientational potential, and which are not sufficiently informative to discriminate between more refined models. Furthermore, recent molecular dynamics simulations on cyanobiphenyls [30], performed at the resolution of the united-atom approximation, seem to support the reliability of the Maier–Saupe model (in terms of the ratio $\langle P_4\rangle/\langle P_2\rangle$ versus the reduced temperature over the whole range of stability of the nematic phase) for such a class of nematic liquid crystals.

On adopting Equation (20) we assume that the molecule in its dynamically-averaged conformation is essentially uniaxial about the z-axis of the MF. This assumption is, however, well accepted and based, for example, on studies of the orientational order of 5CB determined from NMR spectra of partially deuteriated molecules (see, for example, Emsley *et al.* [31] and the data in Table 5 of Emsley *et al.* [32], which gives the values of the ordering matrix elements and shows that the molecular biaxiality is rather small). Consistently, we also take the rotational diffusion tensor, $\mathbf{D}$, to have a diagonal form in the Molecular Frame, with components $D_\parallel$ for spinning around the z-axis and $D_\perp$ for tumbling of the z-axis. It should be stressed here that, according to our choice of MF, the spinning of the molecule about the z-axis is strongly affected by the internal conformational motions, i.e. $D_\parallel$ is only an effective rotational diffusion coefficient.

4. Fit of the relaxation data and interpretation

From the raw experimental data for T_{1Q} and T_{1Z} shown in Figure 4 we have extracted with Equations (7) the angular profiles of $J_1(\theta_B, \omega_0)$ and $J_2(\theta_B, 2\omega_0)$ at the Larmor frequency, $\omega_0 = 46$MHz. The value

$q_{CD} = 165$kHz has been used for the quadrupolar constant of the deuterons in C_α–D bonds. Our goal was to parameterise the global model for ODF and rotational dynamics in order to achieve the best agreement between the experimental and calculated spectral densities at the three temperatures 6°C, 15°C and 25°C studied. Our choice here was to fit *directly* the angular profiles of the spectral densities. However, we stress that these profiles could first be fitted by means of Equations (12) with respect to the six parameters $A_1^{(0)}(\omega_0), A_1^{(2)}(\omega_0), A_1^{(4)}(\omega_0)$ and $A_2^{(0)}(2\omega_0), A_2^{(2)}(2\omega_0)$, $A_2^{(4)}(2\omega_0)$; at a second stage, the values found for these parameters would have to be reproduced by a proper parametrisation of the global model for ODF and rotations of the single molecule. These two procedures are, in principle, equivalent, but the one adopted here is more direct in the sense that it avoids the two-step route. A stronger motivation to use *a priori* the route of the direct matching between model and data is that a pre-fit of the spectral densities with respect to the six parameters is not sensible if the angular dependence of the profiles is weak (this turns out to be the case of the $J_2(\theta_B, 2\omega_0)$ as shown later) and/or if the experimental errors are relevant. In this situation the parameters might be obtained with very different accuracies, or some of them may not even be reliable at all; this would limit the amount of information needed in the subsequent parametrisation of the dynamic model, or it could introduce a bias on the outcome which cannot be easily controlled.

A FORTRAN code has been written to calculate $j_0(\omega)$, $j_1(\omega)$, $j_2(\omega)$ at $\omega = \omega_0$ and $2\omega_0$. The rotational time-correlation functions required to evaluate $j_m(\omega)^{rot}$ have been evaluated by means of a matrix representation of the Smoluchowski operator and its diagonalisation to obtain eigenvalues/eigenvectors (see Domenici *et al.* [33] for details). Normalised Wigner functions have been adopted as an ortho-normal set of basis functions to achieve the matrix representation. Checks on convergence/accuracy of the numerical calculations were made with respect to the enlargement of the set of basis functions. The contribution $j_1(\omega)^{ODF}$ has been estimated by means of Equation (15) for given parameters, as we shall discuss later.

For each temperature, once a value of β_Q is given, the parameter ε is determined from the value of $\langle P_2 \rangle$ calculated from the quadrupolar splitting, $\Delta\nu_0$, measured directly from the spectrum at $\theta_B = 0°$:

$$\langle P_2 \rangle = S_{CD}/P_2(\cos\beta_Q), \quad S_{CD} = \Delta\nu_0/(3q_{CD}/2), \quad (21)$$

where S_{CD} is the order parameter of the C–D bond. Notice that S_{CD} (referred to the DF) is derived here by using Equation (2), that is, by identifying S_{CD} with S_{CD}^0 itself; in the limit of small-amplitude ODF this is a good approximation since ADF and DF are almost coincident.

Due to the large number of free parameters entering the model, a first set of fits has been performed by considering only the molecular tumbling without the ODF. A global fit of J_1 and J_2 has been performed according to the following route/criteria:

(1) The free parameters β_Q, $D_\parallel$ and $D_\perp$ are varied on a grid of values.

(2) From the value of β_Q, the parameter ε is determined by means of Equation (21). The measured values of $\Delta\nu_0$ (see the data in Section 2) are reproduced numerically with ε equal to -2.600 at 25°C, -3.210 at 15°C, and -3.684 at 6°C.

(3) For the current set of these parameters, calculations of J_1 and J_2 at the orientations sampled experimentally are performed. The functions χ_i^2 for the profiles $i = 1, 2$ are evaluated by accounting for the error bars on the data, $\Delta J_i^{exp}(\theta_{B,n})$:

$$\chi_i^2 = \sum_{n=1}^{n°points} \left[\frac{J_i^{exp}(\theta_{B,n}) - J_i^{calc}(\theta_{B,n})}{\Delta J_i^{exp}(\theta_{B,n})} \right]^2, \quad (22)$$

$i = 1$ and 2.

Errors in the spectral densities are estimated by propagating the uncertainties in the measured relaxation times through Equation (7) via

$$\Delta J_1^{exp} = \left| \frac{\partial J_1}{\partial T_{1Q}} \right| \times \Delta T_{1Q} = \frac{\Delta T_{1Q}}{3T_{1Q}^2}$$

and

$$\Delta J_2^{exp} = \left| \frac{\partial J_1}{\partial T_{1Z}} \right| \times \Delta T_{1Z} + \left| \frac{\partial J_2}{\partial J_1} \right| \times \Delta J_1 = \frac{\Delta T_{1Z}}{4T_{1Z}^2} + \frac{\Delta T_{1Q}}{12T_{1Q}^2}. \quad (23)$$

(4) The global error $\chi^2 = \chi_1^2 + \chi_2^2$ is calculated.

(5) The best estimates for β_Q, $D_\parallel$ and $D_\perp$ are those that minimise χ^2 and equalise, as far as possible, χ_1^2 and χ_2^2 in order to avoid a bias due to a preferential weight of J_1 or J_2.

In order to speed up the procedure, a pre-fit with respect to the angle β_Q was made in the following way: $D_\parallel$ and $D_\perp$ have been varied on a wide but distributed grid of values, while β_Q has been varied about the expected value (180°-tetrahedral angle) in steps of 1° between 69° and 76° to achieve the optimal fit. The same value of 74° has been found for all three temperatures, which is slightly larger than that expected

Table 1. Outcome of the global fits of the angular profiles for J_1 and J_2 by excluding the ODF contribution. The value $\beta_Q = 74°$has been fixed at all temperatures.

T/°C	$\langle P_2 \rangle$	$D_\parallel$ /s^{-1}	$D_\perp$ /s^{-1}
25	0.546	2.5×10^9	1.3×10^7
15	0.632	2.3×10^9	2.0×10^7
6	0.683	1.4×10^9	1.2×10^7

from the geometry of the molecule. Such a value was then taken as *fixed* for all the temperatures in the subsequent fits with respect to $D_\parallel$ and $D_\perp$, which were varied on wide grids of values with a thin spacing. A sequence of these fits has been made by further restricting the range of variation of the parameters about the best values. In the final run, the most refined fit was made by varying $D_\parallel$ between $5 \times 10^8 s^{-1}$ and $3.5 \times 10^9 s^{-1}$, and $D_\perp$ between $6 \times 10^6 s^{-1}$ and $3.5 \times 10^7 s^{-1}$, with a homogeneous logarithmic partition into 100 intervals for both variables. Since the route described here is a minimisation of the global χ^2 function via a direct search on a grid, uncertainties in the optimised parameters could not be estimated without arbitrariness.

The outcome of the fits is collected in Table 1 and presented in Figure 6. From the plots we can see that the fit is good at the intermediate temperature of 15°C, while poorer agreement is found at lower and higher temperatures.

For the second stage of the data analysis we have included a theoretical contribution of the ODF, and then repeated the fit with respect to $D_\parallel$ and $D_\perp$, as described previously. In order to have a tentative estimate of $j_1(\omega)^{ODF}$ at the two frequencies, $\omega = \omega_0$ and $\omega = 2\omega_0$, the factor w in Equation (16) has been evaluated by taking $K = 7 \times 10^{-12}$N as the average elastic constant of 5CB at 25°C [34, 35] and $\eta_{eff} = 0.05$ Pa s for the effective viscosity. The resulting value is $w = 2.8 \times 10^{-6}$ s $^{3/2}$. Such an estimate of the effective viscosity is based on the theoretical analysis made in Frezzato *et al.* [36] for low-molecular-weight nematics, where it is demonstrated that η_{eff} can be identified with the bend viscosity whose value is bounded from above by the rotational viscosity γ_1 [19]. By considering experimental estimates of γ_1 for 5CB in the temperature range studied here [37], we find the intermediate value 0.05 Pa s which may be taken as a reasonable guess for the effective viscosity to be employed for all the three temperatures. Values of the short-length cut-off between the extremes of 50 and 100 Å have been considered; these give values for the cut-off function $U(\omega_0/\omega_c)$ between 0.8 and 0.2, respectively. The corresponding values of $\omega_c/2\pi$ are 35 MHz for a short-length of 50 Å and 9 MHz for 100 Å; these are larger than the value employed by Dong in his analysis of transverse relaxation in 5CB [38] but close to estimates for the nematic phase of MBBA [24]. Notice that these choices for λ_c should overestimate the ODF, if we believe that the short-length cut-off should be much longer than the major molecular length (i.e. hundreds of Ångstroms) and taking into account that the cut-off function

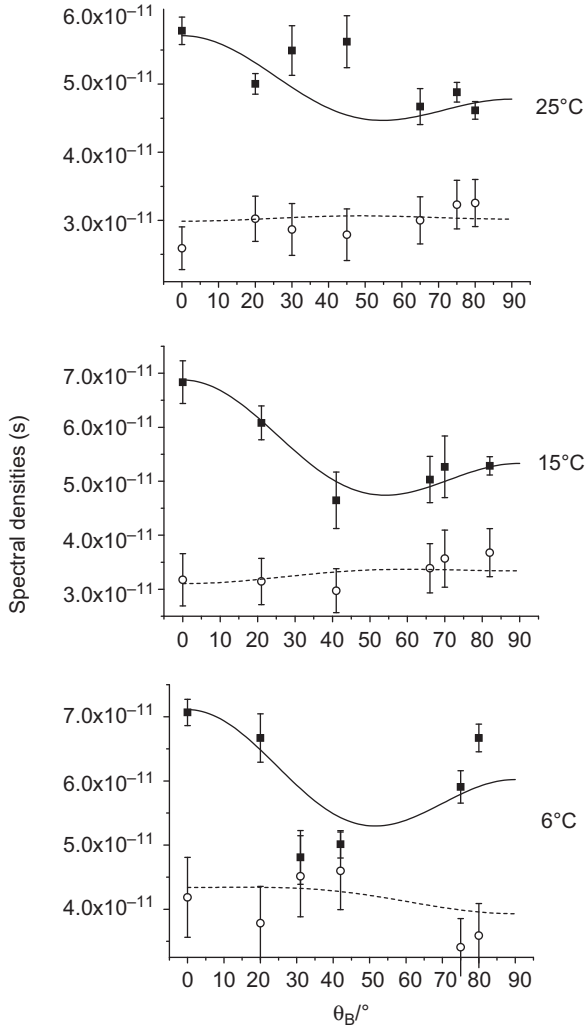

Figure 6. Angular dependence of the spectral densities $J_1(\theta_B, \omega_0)$ and $J_2(\theta_B, 2\omega_0)$ at the three temperatures studied. Experimental data (J_1, filled squares; J_2, open circles). The dashed and full lines correspond to the fitting based on the theoretical analysis described in Section 4.

decreases rapidly as λ_c increases. Just to give an idea of the significance of the ODF with such a parameterisation, they provide an additive contribution to J_1 at $\theta_B = 0^\circ$ of about 10^{-11}s *at most* at 25°C, that is, about 15% of the total amount. From the attempts to fit the data with respect to $D_\parallel$ and $D_\perp$ by including the ODF with this chosen parametrisation (kept fixed), it turns out that there is no improvement to the fit, and that much smaller values of $D_\perp$ would be obtained; this sounds unrealistic. On this basis we conclude that there is no *need* to include a contribution from the ODF, in the sense that they should play a quantitatively minor role with respect to the molecular motions. Moreover, ODF probably contribute *much less* than 15% at $\theta_B = 0^\circ$ in the longitudinal relaxation process. A more pronounced effect of the ODF is found for the transverse (spin-spin) relaxation in 5CB, as revealed by Dong [38]. Analysis of the angular-dependent transverse relaxation rates is currently in progress [23].

From the data fit it turns out that $D_\perp$ is essentially insensitive with respect to changes in temperature in the range 6 to 25 °C. This behaviour is unexpected and deserves further investigation over a wider temperature range and a larger number of intermediate temperatures. Moreover, the value of $D_\perp$ of approximately $\sim 1.5 \times 10^7 s^{-1}$ is close to recent estimates based on molecular dynamics simulations of an atomistic model of 5CB [39] and to the values obtained by Dong from the analysis of spin-spin relaxation (see Table I in Dong [38]). In addition, $D_\parallel$ takes typical values for diffusion coefficients associated with spinning motions of low-molecular-weight mesogens in liquid crystals ($\sim 10^{10} s^{-1}$) [40], and it is in agreement with the estimates obtained by Dong [38] and with recent molecular dynamics simulations [41]. We note that a value for $D_\parallel$ which is about two orders of magnitude higher than $D_\perp$ conflicts with any estimate made using simple scaling laws based on Perrin's model [42] for elongated rigid molecules rotating in a homogeneous viscous environment. Indeed, this model would predict a ratio $D_\parallel/D_\perp$ of the order of only a few units depending on the aspect ratio of the molecule. However, the internal motions are expected to have a large effect, in the sense that $D_\parallel$ is a diffusion coefficient for an effective spinning motion which couples molecular rotations about the symmetry axis with the faster conformational dynamics. In contrast to $D_\perp$, we find that $D_\parallel$ has a clear and continuous temperature dependence. In Figure 7 we show an attempt at an Arrhenius-like plot, based on just three points, from which an activation energy of about 20 kJ/mol was extracted. Such a value lies in the typical range of activation energies for parallel diffusion coefficients [40], and it is, in addition, of the order of magnitude

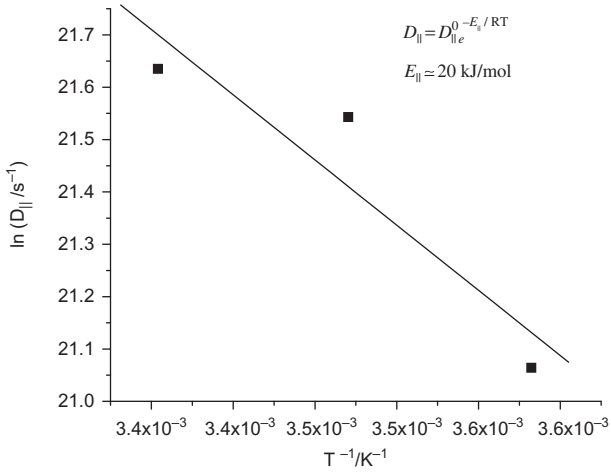

Figure 7. Arrhenius-like plot for the temperature dependence of the parallel diffusion coefficient.

of energy barriers for highly hindered conformational transitions. Clearly, since we have only three temperatures and the relative uncertainty on the activation energy from the Arrhenius plot is close to 50%, such an analysis can only be taken as an indication supporting the picture that activated intramolecular motions contribute to the determination of $D_\parallel$.

5. Outlines and conclusions

In this work we have illustrated how ^{2}H-NMR experiments can be performed on nematic samples oriented with respect to the magnetic field in the spectrometer by applying a competing electric field, and how the orientation-dependent longitudinal relaxation is very informative about the features of single-molecule dynamics. In fact, in the usual experiments with the sample aligned at the canonical orientation only *two values* of the spectral densities, $J_1(\omega_0)$ and $J_2(2\omega_0)$, are obtained while here *two entire angular profiles,* $J_1(\theta_B, \omega_0)$ and $J_2(\theta_B, 2\omega_0)$, related to six independent pieces of information have been determined. These offer the possibility to perform a much more reliable data fit with respect to the model parameters and to validate the assumed dynamic model as well.

In particular, we have focused here on longitudinal spin relaxation of the nematogen 5CB specifically deuteriated in the alpha position of the pentyl chain. We have adopted a minimal model for the dynamics, where ODF and single-molecule rotations with respect to the local director are dynamically decoupled, and by assuming that the internal conformational motions are very fast. The analysis of the experimental data has allowed us (a) to establish that ODF do not contribute significantly to the longitudinal relaxation, probably

much less than 15%; (b) to demonstrate that the model of small-step diffusion in a Maier–Saupe potential is suitable for the description of the molecular rotational dynamics; and (c) to estimate the rotational diffusion coefficients $D_\perp$ (tumbling motion) and $D_\parallel$ (effective spinning motion). Both parameters are in agreement with previous estimates. However, a temperature-independent $D_\perp$ is found; this unexpected feature should be investigated further.

Future work on the specifically deuteriated 5CB sample will deal with the analysis of the transverse spin relaxation rate, namely the decay rate of the Quadrupolar Echo versus the evolution delays between radiofrequency pulses in the sequence, in order to build up a self-consistent methodology to investigate the dynamical features by means of two independent ^{2}H-NMR experiments.

Acknowledgements

The authors thank the Royal Society for the grant awarded through the "International Joint Project IJP-2005/R4", *NMR Investigation of Translational and Rotational Dynamics in Liquid Crystals*, 2006–2009.

References

[1] Ferrarini, A.; Nordio, P.L.; Moro, G.J. In *The Molecular Dynamics of Liquid Crystals*: Luckhurst, G.R., Veracini, C.A., Eds.; Kluwer Academic: Dordrecht, The Netherlands, 1994; pp 41–49.
[2] Luckhurst, G.R. *J. Chem. Soc. Faraday Trans.* **1988**, *84*, 961–986.
[3] Dong, R.Y. *Nuclear Magnetic Resonance of Liquid Crystals*, 2nd ed.; Springer-Verlag: New York, 1997.
[4] Dong, R.Y. *Progr. Nucl. Magn. Reson. Spect.* **2002**, *41*, 115–151.
[5] Abragam, A. *Principles of Nuclear Magnetism*; Oxford University Press: New York, 1961.
[6] Slichter, C.P. *Principles of Magnetic Resonance*, 3rd ed.; Spinger-Verlag: Berlin, 1990.
[7] Ferrarini, A.; Moro, G.J.; Nordio, P.L. *Mol. Phys.* **1988**, *63*, 225–247.
[8] Nordio, P.L.; Busolin, P. *J. Chem. Phys.* **1971,** *55,* 5485–5491; Nordio, P.L.; Rigatti, G.; Segre, U. *J. Chem. Phys.* **1971,** *56,* 2117–2123.
[9] Frezzato, D.; Kothe, G.; Moro, G.J. *J. Phys. Chem. B* **2001,** *105,* 1281–1292; Frezzato, D.; Moro, G.J.; Kothe, G. *J. Chem. Phys*. **2003,** *119,* 6931–6945; Frezzato, D.; Kothe, G.; Moro, G.J. *J. Chem. Phys*. **2003,** *119,* 6946–6958.
[10] Catalano, D.; Cifelli, M.; Geppi, M.; Veracini, C.A. *J. Phys. Chem. A* **2001**, *105*, 34–40.
[11] Domenici, V.; Geppi, M.; Veracini, C.A.; Blinc, R.; Lebar, A.; Zalar, B. *Chem Phys Chem* **2004**, *5*, 559–563.
[12] Kimmich, R.; Anoardo, E. *Progr. Nucl. Magn. Reson. Spect*. **2004**, *44*, 257–320.
[13] Barbara, T.M.; Vold, R.R.; Vold, R.L. *J. Chem. Phys.* **1983**, *79*, 6338–6340.
[14] Cifelli, M.; Forte, C.; Geppi, M.; Veracini, C.A. *Mol. Cryst. Liq. Cryst.* **2002**, *372*, 81–95.
[15] Tarr, C.E.; Nickerson, A.A.; Smith, C.W. *Appl. Phys. Lett.* **1970,** *17,* 318–320; Tarr, C.E.; Fuller, A.M.; Nickerson, M.A. *Appl. Phys. Lett.* **1971,** *19,* 179–182.
[16] Doane, J.W.; Tarr, C.E.; Nickerson, M.A. *Phys. Rev. Lett.* **1974**, *33*, 620–624.
[17] Luckhurst, G.R.; Miyamoto, T.; Sugimura, A.; Timimi, B.A. *J. Chem. Phys*. **2002**, *117*, 5899–5907.
[18] Gray, G.W.; Harrison, K.J.; Nash, J.A. *Electron. Lett.* **1973**, *9*, 130–131.
[19] de Gennes, P.G.; Prost, J. *The Physics of Liquid Crystals*, 2nd ed.; Clarendon Press: Oxford, 1993.
[20] Wimperis, S. *J. Magn. Reson.* **1990**, *86*, 46–59.
[21] Beckmann, P.A.; Emsley, J.W.; Luckhurst, G.R.; Turner, D.L. *Mol. Phys.* **1983**, *50*, 699–725.
[22] Counsell, C.R.J.; Emsley, J.W.; Luckhurst, G.R.; Turner, D.L.; Charvolin, J. *Mol. Phys.* **1984**, *52*, 499–503.
[23] Unpublished results; the analysis is currently in progress by the authors.
[24] Dong, R.Y.; Shen, X. *J. Phys. Chem. A* **1997**, *101*, 4673–4678.
[25] Rose, M.E. *Elementary Theory of Angular Momentum*; John Wiley & Sons, Inc.: New York, 1957.
[26] Luckhurst, G.R.; Sanson, A. *Mol. Phys.* **1972,** *24,* 1297–1311; Luckhurst, G.R.; Zannoni, C. *Proc. Roy. Soc. A* **1977,** *352,* 87–102.
[27] Vold, R.L.; Vold, R.M.; Warner, M. *J. Chem. Soc. Faraday Trans. 2* **1988**, *84*, 997–1013.
[28] Joghems, E.A.; van der Zwan, G. *J Phys. II France* **1996**, *6*, 845–871.
[29] Gardiner, C.W. *Handbook of Stochastic Methods*; Springer: Berlin, 1994.
[30] Tiberio, G.; Muccioli, L.; Berardi, R.; Zannoni, C. *Chem Phys Chem* **2009,** *10,* 125–136.
[31] Emsley, J.W.; Luckhurst, G.R.; Gray, G.W.; Mosley, A. *Mol. Phys.* **1978**, *35*, 1499–1503.
[32] Emsley, J.W.; Luckhurst, G.R.; Stockley, C.P. *Mol. Phys.* **1981**, *44*, 565–580.
[33] Domenici, V.; Frezzato, D.; Veracini, C.A. *J. Phys. Chem. B* **2006**, *110*, 24884–24896 (see supporting information).
[34] Bunning, J.D.; Faber, T.E.; Sherrell, P.L. *J. Physique* **1981**, *42*, 1175–1182.
[35] Dunmur, D.A., Fukuda, A., Luckhurst, G.R., Eds. *Physical Properties of Liquid Crystals: Nematics*; EMIS Datareviews Series No. 25, INSPEC Publication, 2001; Ch 5.2.
[36] Frezzato, D.; Kothe, G.; Moro, G.J. *Mol. Cryst. Liq. Cryst.* **2003**, *394*, 107–118.
[37] Wu, S.-T.; Wu, C.-S. *Phys. Rev. A:At., Mol., Opt. Phys.* **1990**, *42*, 2219–2227.
[38] Dong, R.Y. *Phys. Rev. E: Stat., Nonlinear Soft Matter Phys.* **1998**, *57*, 4316–4322.
[39] Ilk Capar, M.; Cebe, E. *Chem. Phys. Lett.* **2005**, *407*, 454–459.
[40] Richardson, R.M. In *Handbook of Liquid Crystals – Fundamentals*: Demus, D., Goodby, J., Gray, G.W., Eds.; Wiley – VCF, 1998; Ch. 4.
[41] Cifelli, M.; De Gaetani, L.; Prampolini, G.; Tani, A. *J. Phys. Chem. B* **2008**, *112*, 9777–9786.
[42] Perrin, P.F. *J. Phys. Radium* **1934**, *5*, 497–591; **1936**, *7*, 1–11.